Applied Geography 55 (2014) 165–175

Contents lists available at ScienceDirect

Applied Geography

journal homepage: www.elsevier.com/locate/apgeog

Characterizing recent and projecting future potential patterns of mountain pine beetle outbreaks in the Southern Rocky Mountains

Lu Liang [a], Todd J. Hawbaker [b], Yanlei Chen [a], Zhiliang Zhu [c], Peng Gong [a, d, e, *]

[a] *Department of Environmental Science, Policy and Management, University of California, Berkeley, CA 94720, USA*
[b] *Geological Survey, P.O. Box 25046, DFC, MS 980, Denver, CO 80225, USA*
[c] *U.S. Geological Survey, 12201 Sunrise Valley Drive, Reston, VA 20192, USA*
[d] *Ministry of Education Key Laboratory for Earth System Modeling, Center for Earth System Science, Tsinghua University, Beijing, China*
[e] *Joint Center for Global Change Studies, Beijing 100875, China*

ARTICLE INFO

Article history:
Available online 29 September 2014

Keywords:
Mountain pine beetle
Landsat
General linear model
Climate change
Remote sensing

ABSTRACT

The recent widespread mountain pine beetle (MPB) outbreak in the Southern Rocky Mountains presents an opportunity to investigate the relative influence of anthropogenic, biologic, and physical drivers that have shaped the spatiotemporal patterns of the outbreak. The aim of this study was to quantify the landscape-level drivers that explained the dynamic patterns of MPB mortality, and simulate areas with future potential MPB mortality under projected climate-change scenarios in Grand County, Colorado, USA. The outbreak patterns of MPB were characterized by analysis of a decade-long Landsat time-series stack, aided by automatic attribution of change detected by the Landsat-based Detection of Trends in Disturbance and Recovery algorithm (LandTrendr). The annual area of new MPB mortality was then related to a suite of anthropogenic, biologic, and physical predictor variables under a general linear model (GLM) framework. Data from years 2001–2005 were used to train the model and data from years 2006–2011 were retained for validation. After stepwise removal of non-significant predictors, the remaining predictors in the GLM indicated that neighborhood mortality, winter mean temperature anomaly, and residential housing density were positively associated with MPB mortality, whereas summer precipitation was negatively related. The final model had an average area under the curve (AUC) of a receiver operating characteristic plot value of 0.72 in predicting the annual area of new mortality for the independent validation years, and the mean deviation from the base maps in the MPB mortality areal estimates was around 5%. The extent of MPB mortality will likely expand under two climate-change scenarios (RCP 4.5 and 8.5) in Grand County, which implies that the impacts of MPB outbreaks on vegetation composition and structure, and ecosystem functioning are likely to increase in the future.

Introduction

As a native species, mountain pine beetle (*Dendroctonus ponderosae*; MPB) populations have existed at endemic levels and periodically have grown to epidemic levels in the pine forests of western North America for centuries (Amman, 1977; Baker & Veblen, 1990; Raffa et al., 2008). By infesting and killing older and stressed trees with larger diameters, MPB plays a critical role in shaping forest composition and structure, accelerating the movement of nutrients in biogeochemical cycles, and affecting forest productivity (Collins, Rhoades, Hubbard, & Battaglia, 2011; Edburg et al., 2012). In recent decades this historical balance has been disrupted, and the area affected by MPB has been vastly extended, exceeding the extent and impacts of outbreaks documented in the past 125 years (Raffa et al., 2008). The current MPB outbreak has impacted large expanses of lodgepole and ponderosa pine forests, reduced their ability to act as carbon sinks (Caldwell, Hawbaker, Briggs, Cigan, & Stitt, 2013; Kurz et al., 2008; Running, 2008), altered wildfire hazards (Hicke et al., 2012; Jenkins, Hebertson, Page, & Jorgensen, 2008; Parker, Clancy, & Mathiasen, 2006; Schoennagel, Veblen, Negron, & Smith, 2012), modified local surface energy balance (Boon, 2009), threatened water quality (Mikkelson et al., 2013), and changed regional climate (Maness, Kushner, & Fung, 2013).

---

[*] Corresponding author. Ministry of Education Key Laboratory for Earth System Modeling, Center for Earth System Science, Tsinghua University, Beijing 100084, China.

E-mail address: penggong@berkeley.edu (P. Gong).

http://dx.doi.org/10.1016/j.apgeog.2014.09.012

The population dynamics of bark beetles are governed by a variety of biotic and abiotic factors and their interactions (Raffa et al., 2008). Forest characteristics, including homogenous even-aged, high-density, and large-diameter stands, are favorable for MPB mass attack (Raffa & Berryman, 1983). Long-term drought or other events causing stress can exert either positive or negative effects on tree susceptibility to beetle attack, and the overall impact remains controversial. While the primary defense mechanism of trees will be weakened by drought stress because of reduced resin quantities (Creeden, Hicke, & Buotte, 2014; Preisler, Hicke, Ager, & Hayes, 2012; Raffa et al., 2008), beetle brood production can also be reduced since the tree's phloem thickness is attenuated (Amman & Cole, 1983). Thermal regimes, typically represented by minimum winter temperature or year-round temperature, impact beetles' developmental timing, cold-induced mortality, and the associated fungal community (Bentz et al., 2010; Preisler et al., 2012). Meanwhile, factors like elevation, direct solar radiation, and beetle mortality in adjacent areas have also been indicated as important predictors of outbreaks (Coops, Wulder, & White, 2006; Simard, Powell, Raffa, & Turner, 2012; Walter & Platt, 2013; Wulder, White, Bentz, Alvarez, & Coops, 2006). Most previous studies have focused on the effects of one or several factors. In this study, we took a comprehensive approach and considered a large set of relevant factors to improve our understanding of the spatiotemporal patterns of MPB outbreaks and investigate their drivers.

For this study, we were also concerned about the identification of forested areas with high risk for future MPB mortality. There have been a number of prior efforts to predict patterns of MPB mortality. Through an integrated seasonality and cold tolerance model, Bentz et al. (2010) suggested that rising temperatures could increase MPB population growth rates, and their range would expand along latitude and elevation gradients. Aided by an ecological niche model, Evangelista, Kumar, Stohlgren, and Young (2011) predicted that new areas of forest susceptible to MPB mortality would emerge over time but the existing area of susceptible forests to MPB mortality would also shrink, leading to an overall decrease in the amount of suitable habitat area for MPB in the future. Using a process-based model, Hicke, Logan, Powell, and Ojima (2006) found that projected warming in the western United States will result in substantial reductions in the overall area of adaptive seasonality (the synchronous emergence of adults that allows MPB to overwhelm tree defenses). Unlike population models, which can improve the mechanistic understandings of biological responses to environmental variability, but may consider a limited number of explanatory variables because of model complexity, statistical approaches are capable of incorporating a large number of explanatory variables and quantifying their relative roles. This is a crucial preliminary step before adopting and improving process-based mechanistic models.

Understanding the factors driving patterns of MPB outbreaks and predicting future outbreaks has been challenging given the types of data available that depict the spatial and temporal extents of outbreaks. The quality of response variables could affect the performance of predictive models. In general, locations of MPB mortality are collected in the field or extracted from remotely sensed imagery. Although in-situ surveys can provide accurate data, they often have restricted geographic and temporal coverage. State and federal agencies have conducted Forest Health Monitoring Aerial Detection Surveys (ADS) to identify forest disturbances since the mid-twentieth century (Man, 2010). These publicly available datasets have been used extensively in many fields, but errors introduced via observer fatigue, observer-to-observer variation, misregistration and the scale of observation (Meigs, Kennedy, & Cohen, 2011) are rarely estimated and could introduce an unknown amount of uncertainty.

Remote sensing of forest disturbances offers an alternative to the ADS data for monitoring tree mortality caused by insect outbreaks (Coops et al., 2006; White, Wulder, Brooks, Reich, & Wheate, 2004). Landsat data are especially popular for this application because they are freely available, and have multispectral data, a broad spatial extent, and temporal continuity. For these reasons, Landsat time series stacks (LTSS) have been used in large-scale efforts to detect forest disturbances (Masek et al., 2013) using the Vegetation Change Tracker algorithm (VCT; Huang et al., 2010). Remotely sensed disturbance maps produced by VCT and similar change-detection algorithms like the Landsat-based Detection of Trends in Disturbance and Recovery algorithm (LandTrendr; Kennedy, Yang, & Cohen, 2010) currently lack information about the cause of the disturbance, and that limits their utility for use in our study. Notwithstanding, several studies have demonstrated the usefulness of Landsat in capturing the patterns of MPB-caused tree mortality at various geographic scales (e.g. Masek et al., 2013; Meddens, Hicke, Vierling, & Hudak, 2013). Considering the uncertainties in the ADS data, and limitations of existing VCT and LandTrendr change-detection products, we utilized data from an automated procedure that labeled disturbance types (especially MPB mortality) detected by LandTrendr in an LTSS to generate spatially explicit annual maps of MPB occurrences over a decade-long time span (Liang, Chen, Hawbaker, Zhu, & Gong, 2014).

In this paper, we integrated remote sensing techniques and statistical models to evaluate the effects of a set of factors affecting the dynamic pattern of MPB mortality, and projected future MPB mortality in response to climate change. Our aim was to address the following questions: What drivers promote the extensive development and progressive MPB outbreak in an area situated in the Southern Rocky Mountains ecoregion? How accurately can we predict MPB disturbance with this set of response and explanatory variables? And what will future outbreak trends be?

Methods

Study area

Grand County is located in north central Colorado, covering approximately 4830 square kilometers of the Southern Rocky Mountains ecoregion (Fig. 1). The elevation ranges from 2225 m along the Colorado River to 4131 m at the summit of the Continental Divide (Grand County Department of Natural Resources, 2006). Its climate is characterized by year-round sunny days (around 244 days/year on average), with average summer temperatures of 26.6 °C, and the average rainfall of approximately 30.48 cm (Grand County Department of Natural Resources, 2006). The diversity of elevation, soil, climate, as well as strong topographic-moisture gradients leads to a variety of vegetation composition within the county, among which sagebrush shrub and steppe is the most dominant ecosystem. Lodgepole pine forests occupy a quarter of the landmass, followed by spruce-fir forests and aspen forests (Grand County Department of Natural Resources, 2006). In recent decades, MPB infestation, wildfire, and timber harvesting are recognized as the three major disturbance agents in Grand County. Wildfire occurrence has been low, but the widespread MPB outbreak affected approximately 68% of privately owned land and 70% of federally owned land (Witcosky, 2007).

Change detection analysis in detecting long-term MPB outbreaks

Maps of MPB mortality in Grand County were generated by automatic attribution of LandTrendr segmentation outputs applied to a time series of 17 Landsat images spanning 2000–2011 (path 34, row 32; Liang et al., 2014). This approach integrated a temporal

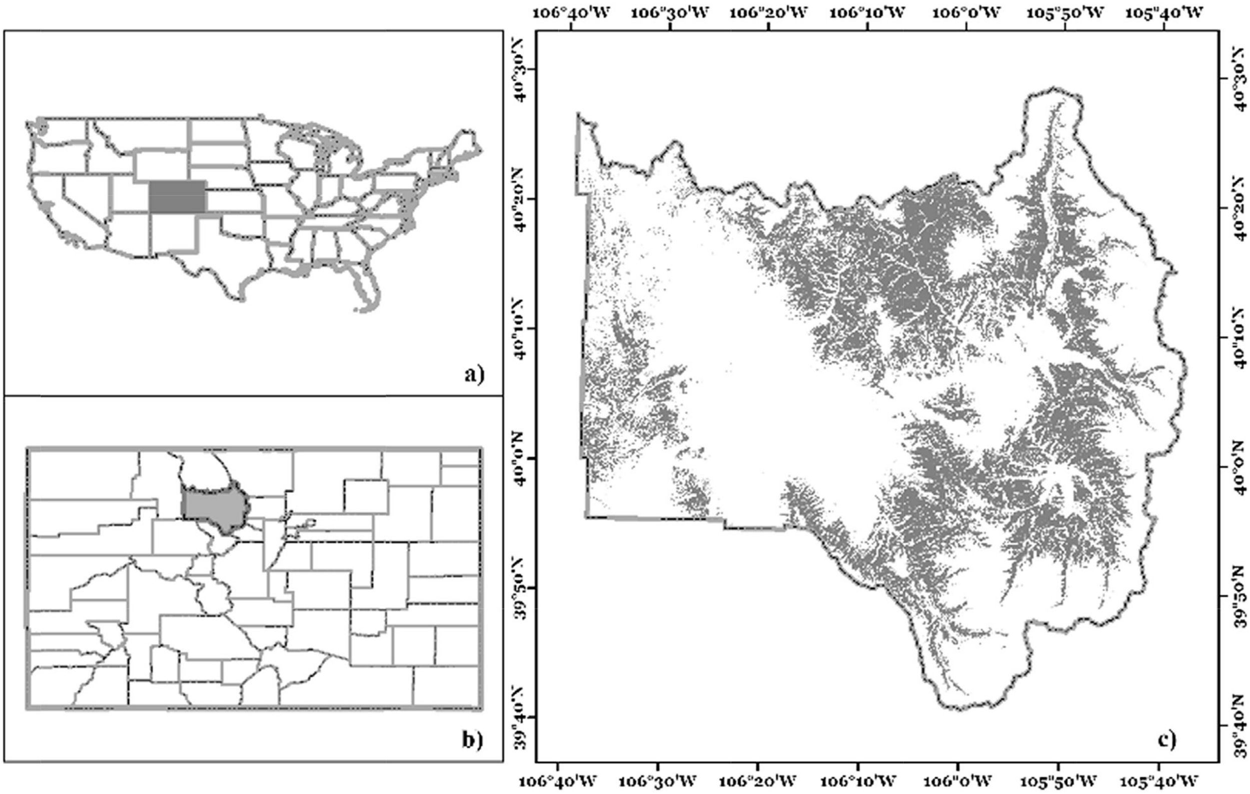

Fig. 1. Spatial location of (a) the State of Colorado within the United States of America, (b) Grand County within Colorado, and (c) areas of lodgepole pine forest (derived from the LANDFIRE existing vegetation type data layer) within Grand County, Colorado.

segmentation technique to identify areas with change (Kennedy et al., 2010) and a decision tree modeling procedure to attribute the changes to specific disturbance types (Liang et al., 2014). The steps in this approach were to enhance the signal-to-noise ratio of the time series curve via linear regressions, and decompose it into a sequence of straight-line segments, whose event attributes were identified based on the segment characteristics (duration, magnitude and vertex value) using calibrated decision tree rules (Fig. 2). The temporal trajectories were constructed using the Normalized Burn Ratio (Key & Benson, 2006). Key parameters that were used to calibrate both temporal segmentation and decision tree components were trained using ground-truth data from 106 sample locations, visually selected and interpreted from 1-m resolution U.S. Department of Agriculture (USDA) National Agricultural Imagery Program (NAIP) imagery (available in 2005, 2009, and 2011 from USDA Geospatial Data Gateway). Technical details can be found in Liang et al. (2014). The trend analysis outputs included a series of disturbance maps that depict healthy forest, forest with MPB mortality, and clearcut areas at an annual time step. The disturbance maps were validated with a set of randomly placed NAIP test samples in Liang et al. (2014).

Model development

Response variable

We were interested in simulating the spread of MPB mortality into new regions over time, instead of modeling their suitable habitats. Thus, we set the response variable in our models to be the annual presence (case) of new MPB mortality and absence (control) of MPB mortality, where presence refers to the new mortality in a pixel which was healthy in the previous year. The time-series of disturbance maps were used as the base for sample selection. First, we made a random sample of newly emerged areas of MPB mortality stratified by each year from 2001 to 2011. A stratum containing persistently (2001–2011) healthy forest pixels was also constructed for control sample selection. Second, since the sample

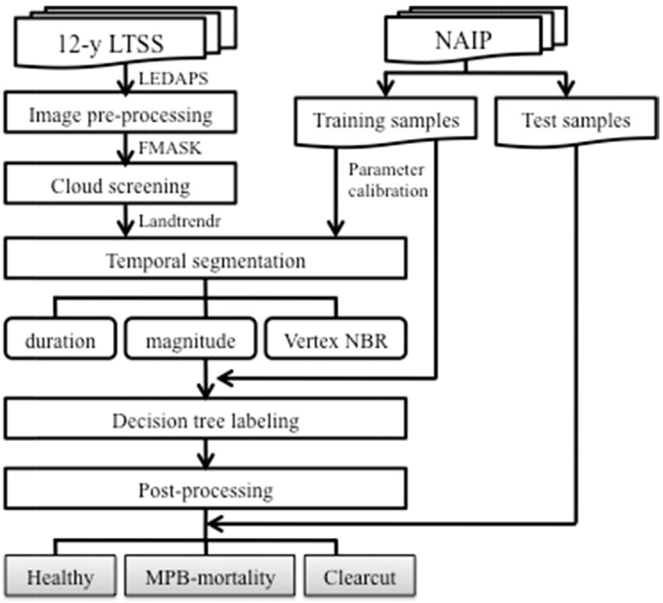

Fig. 2. Processing steps in the change-detection analysis. LTSS: Landsat time-series stacks; NAIP: National Agricultural Imagery Program; LEDAPS: Landsat Ecosystem Disturbance Adaptive Processing System; FMASK: Function of Mask; LandTrendr: Landsat-based Detection of Trends in Disturbance and Recovery algorithm; NBR: Normalized Burn Ratio; MPB: mountain pine beetle.

size in each stratum determines the distance between observations, and thus affects the potential for spatial autocorrelation to influence model interpretation, we initially selected 300 sample units from each stratum, and successively decreased the sample size with decrements of 10. For each sample size, a general linear model (GLM) was fit and Moran's *I* was calculated to test for spatial autocorrelation in the model residuals (Moran, 1950). We ultimately selected the largest sample size that had insignificant spatial autocorrelation in the model residuals, that is, we selected a sample with enough spacing between points so that spatial autocorrelation effects were avoided.

A set of training samples was extracted using observations from 2001 to 2005, and the model with forward predictions was validated with observations from 2006 to 2011. Year 2000 was not included in modeling because we could not infer its prior information for certain predictors, such as distance to nearest cell with MPB mortality in the previous year. Validation data collected after 2008, when spread of the MPB outbreak was reduced, were used to determine whether or not the model over predicted MPB mortality.

Explanatory variables

Thirty-four biotic and abiotic variables that fell into seven categories were used to develop a number of GLMs (Table 1). All datasets, except for the two climate variables, were in raster format with the same spatial resolution as our disturbance maps (30 m). The values from all the rasters were extracted at the locations of the training or validation sample points.

Anthropogenic variables included residential housing density and distance to nearest road. Both of them are proxies for the intensity of human activities, whose impacts have rarely been investigated in prior MPB associated studies. The biggest human impact on forest ecosystems is likely to be habitat fragmentation since silvicultural treatments, such as thinning or logging, are still the most common management strategy in mitigating MPB outbreaks (Coops, Timko, Wulder, White, & Ortlepp, 2008). How human intervention affects MPB host selection remains unknown, however. To quantify the magnitude of this potential effect, we used residential housing density data from the 2010 U.S. Census Bureau block-level housing-density data (Radeloff et al., 2010), and distance to nearest road from the National Overview Road Metric Euclidean Distance dataset (Watts et al., 2007). Both continuous variables were log + 1 transformed prior to use because they had skewed distributions.

Lodgepole pine forests exist along a topographic-moisture gradient that controls vegetation growth as a function of soil water holding capacity, evapotranspiration and surface runoff. Six topographic variables derived from the Shuttle Radar Topography Mission Digital Elevation Model were used to represent this gradient (USGS, 2004). Aspect was recalculated in a way that the first 45° from true north to east was recorded as 1, and increased by 1 as the aspect increased every 45° clockwise. Southwestness is a cosine-transformation of aspect that ranges from −1 to 1 (Franklin, McCullough, & Gray, 2000). Topographic wetness index (TWI) is the steady-state humidity index (Beven & Kirkby, 1979). Higher TWI values indicate greater soil moisture, and we expected TWI and the distance to stream channel networks to be negatively correlated with MPB mortality.

We used tree cover prior to the MPB outbreak as a proxy for the pre-disturbance health and abundance of MPB host species. The

Table 1
Predictor variables selected for use in the general linear models (GLMs).

Category	Variables	Abbreviation	Resolution	Unit
1. Anthropogenic	Distance to the nearest road	road	30 m	m
	Residential housing density	house	30 m	m
2. Topography	Elevation	dem	30 m	m
	Aspect	aspect		Degree
	Slope	slope		Degree
	Southwestness	sw		No unit
	Topographic Wetness Index	twi		No unit
	Distance to the nearest channel network	dis2chan		m
3. Vegetation condition	Tree cover	tc	30 m	Percentage
4. Spatial proximity	Distance to closest mortality in the previous year	dis2prev	30 m	m
5. Neighborhood mortality	Number of pixels in an 8-pixel neighborhood with MPB mortality in the previous year	nm_30m		No unit
	Number of pixels in a 100 m circular neighborhood with MPB mortality in the previous year	nm_100m		No unit
	Same as above, but in a 250 m circular neighborhood	nm_250m		No unit
	Same as above, but in a 500 m circular neighborhood	nm_500m		No unit
	Same as above, but in a 1 km circular neighborhood	nm_1km		No unit
	Same as above, but in a 1500 m circular neighborhood	nm_1500m		No unit
	Same as above, but in a 2 km circular neighborhood	nm_2km		No unit
	Same as above, but in a 3 km circular neighborhood	nm_3km		No unit
6. Climate	Summer mean temperature[a]	tmean_summer	4 km	°C
	Winter mean temperature[a]	tmean_winter		°C
	Summer mean precipitation	ppt_summer_cur		°C
	Warmest temperature	Tmax_cur		°C
	Coldest temperature from October to May	Tmin_cur		°C
	Mean annual temperature of previous year	tmean_last		°C
	Mean annual precipitation of previous year	ppt_mean_last		mm
	Mean summer precipitation of previous year	ppt_summer_last		mm
7. Climate anomalies	Mean summer precipitation anomaly	ppt_summer_cur2normal	4 km	mm
	Mean winter temperature anomaly	tmean_winter2normal		°C
	Warmest temperature anomaly	tmax_cur2normal		°C
	Coldest temperature anomaly	tmin_cur2normal		°C
	Mean annual precipitation anomaly of previous year	ppt_mean_last2normal		mm
	Mean annual temperature anomaly of previous year	tmean_last2normal		°C
	Mean summer temperature anomaly of previous year	tmean_summer2normal		°C
	Mean summer precipitation anomaly of previous year	ppt_summer_last2normal		mm

[a] Summer is from June through August, and winter is from December through February.

Landsat vegetation continuous fields tree cover layer for circa-2000 provides estimates of the aboveground woody vegetation percentage in each 30 m pixel (Sexton et al., 2013). Under most circumstances, canopy cover is positively and significantly correlated with diameter at breast height (Gill, Biging, & Murphy, 2000), and thus high canopy cover usually represents large-diameter trees, which are more likely to be attacked by MPB (Amman, 1977; Klutsch et al., 2009).

Spatial proximity to areas previously affected by MPB can be a critical facilitator in driving local outbreaks because MPB is a relatively poor disperser (Simard et al., 2012), and we included two types of dispersal-related variables to represent it. Distance to nearest mortality is computed as the Euclidean distance from one cell to its closest cell with MPB mortality in the previous year. Shorter distance between sites enhances their connectivity, and thus increases the probability of beetle dispersal to adjacent healthy sites.

Neighborhood mortality is the amount of adjacent pixels with MPB mortality in the previous year. Because spatial synchrony is prevalent among beetle populations during epidemic years (Aukema et al., 2006), more beetle presence in the immediate neighborhood increases the likelihood of a mass attack on adjacent healthy forest. The scale of neighborhood depends on the beetles' dispersal pattern, which has been summarized into two modes: short-distance and long-distance dispersal. Short-distance dispersal happens within stands (Safranyik, Silversides, McMullen, & Linton, 1989), and long-distance dispersal usually occurs when beetles are transported above the forest canopy by wind (de la Giroday, Carroll, Lindgren, & Aukema, 2011; Jackson, Straussfogel, Lindgren, Mitchell, & Murphy, 2008; Robertson, Nelson, & Boots, 2007; Robertson, Nelson, Jelinski, Wulder, & Boots, 2009). The common distances in the short-distance range dispersal are 30–50 m (Robertson et al., 2007; Safranyik et al., 1989; Safranyik, Linton, Silversides, & McMullen, 1992), whereas the long-distance flight dispersal that depends on the wind speed, preflight weight, flight duration, and lipid content (Evenden, Whitehouse, & Sykes, 2014) can be more variable, ranging from several to tens of kilometers. In field observations, 2–3 km were commonly found to be the maximum distance beetles can disperse by entering a new stand from surrounding areas (Robertson, Wulder, Nelson, & White, 2008; Robertson et al., 2009), whereas laboratory flight mill bioassay showed that the mean MPB flight distance ranged between 2.12 and 5.95 km (Evenden et al., 2014). Since there is no consensus about which mode is more important in driving the beetle expansion, we defined a number of neighborhood distances: 30 m, 100 m, 250 m, 500 m, 1 km, 1.5 km, 2 km and 3 km. Those distances were used as the radius of a circular window, and all pixels with MPB mortality in the previous year covered by this window would then be counted to be the neighborhood mortality value for the center cell.

We used climate datasets generated by the Parameter-evaluation Regressions on Independent Slopes Model (PRISM Climate Group, 2010) in which monthly and annual weather data are available at a resolution of approximately 4 km (Daly, Gibson, Taylor, Johnson, & Pasteris, 2002). Besides annual mean temperature and precipitation information in the PRISM data, we derived six additional variables that are controlling factors in the beetles' life cycle (Kaufmann et al., 2008): summer mean temperature, winter mean temperature, summer mean precipitation, warmest summer temperature, coldest winter temperature, and summer mean precipitation in the previous year. Additionally, we computed eight climate anomalies by taking the differences between each climate variable and their 30-year averages from 1981 to 2010, since climate change has been indicated to have both direct and indirect impact on MPB outbreaks (Kurz et al., 2008).

Modeling approach

We used general linear models (GLM) with a logit link and binary response to identify which variables explained recent patterns of MPB mortality and assess potential new areas of MPB mortality. We first applied univariate GLMs to each of the 28 predictor variables to assess their individual relationship with MPB mortality. These models were evaluated by their coefficient estimates and associated significance tests. Their spatial autocorrelation effects were examined using Moran's I on the model residuals. Variables with p-values greater than 0.05 on the spatial autocorrelation tests were excluded from further analyses, to avoid violation of the assumption of independently and identically distributed errors in GLMs (Dormann et al., 2007). We then fit a full model starting with all predictor variables that were not removed because of spatial autocorrelation in the univariate models. We retained statistically significant predictor variables in the full model based on the Bayesian Information Criterion (BIC) in a multiple backward stepwise selection algorithm implemented in R (R Core Team, 2013). We chose BIC because of the large number of predictor variables and BIC penalizes the number of parameters more strongly than commonly used Akaike Information Criterion.

Predictive maps of MPB mortality were generated using the final GLM after backward stepwise selection with the equation:

$$P = 1/(1 + \exp(-(\beta_0 + \beta_1 X_1 + \beta_2 X_2 + \cdots + \beta_i X_i + C)))$$

where P is the probability of MPB mortality, β_0 is the intercept, X_i is a predictor variable, and β_i is the regression coefficient estimate for the associated predictor variable X_i. The correction factor (C) was used to account for model bias introduced because of different ratios of case and control observations in the sample and in the population (Manly, McDonald, Thomas, McDonald, & Erickson, 2002):

$$C = \log\left(\frac{\#\ \text{sample.control}/\#\ \ \text{pop.control}}{\#\ \text{sample.case}/\#\ \text{pop.case}}\right)$$

where # sample.control and # pop.control are the number of healthy (no MPB mortality) occurrences in the sample and the population, respectively; # sample.case and # pop.case are the number of observations with MPB mortality in the sample and the population, respectively.

Model performance evaluation

Model performance was evaluated in three ways. (1) The new presence of MPB mortality each year predicted by our GLM was visually compared with observed MPB mortality in the Landsat classifications. This provided an immediate and intuitive way to perform the evaluation. (2) The areal estimates of MPB mortality derived from remote sensing and GLM were compared and their accuracy was evaluated against the criteria: the peak of tree mortality should occur around 2005 and 2008 (Klutsch et al., 2009), and the rate of change should be the greatest at the beginning and then reduced until reaching a stable level. (3) A quantitative accuracy assessment was also conducted. First, 10-fold cross-validation was applied to test the model performance in the training phases to avoid problems like overfitting. Second, to determine the model's predictive capacity, predicted MPB mortality was compared with an independent dataset extracted from the base maps from 2006 to 2011 in two ways. A set of 3000 points were randomly picked for areas of healthy forest and MPB mortality from the base image of each year, in order to provide an overall evaluation of landscape-level patterns. Another set of 3000 points were selected from areas of persistent healthy forest and new MPB mortality each year,

Table 2
The 14 global climate models (GCMs) from which downscaled climate projections were used in this paper and the modeling groups developing them.

Model name	Modeling group
BCC-CSM1.1	Beijing Climate Center, China Meteorological Administration
BNU-ESM	College of Global Change and Earth System Science, Beijing Normal University
CanESM2	Canadian Centre for Climate Modelling and Analysis
CNRM-CM5	Centre National de Recherches Météorologiques/Centre Européen de Recherche et Formation Avancée en Calcul Scientifique
CSIRO-Mk3.6.0	Commonwealth Scientific and Industrial Research Organization in collaboration with Queensland Climate Change Centre of Excellence
GFDL-ESM2G	National Oceanic and Atmospheric Administration
GFDL-ESM2M	Geophysical Fluid Dynamics Laboratory
HadGEM2-ES	Met Office Hadley Centre (additional HadGEM2-ES realizations contributed by Instituto Nacional de Pesquisas Espaciais)
HadGEM2-CC	
INM-CM4	Institute for Numerical Mathematics
MIROC5	Atmosphere and Ocean Research Institute (The University of Tokyo), National Institute for Environmental Studies, and Japan Agency for Marine-Earth Science and Technology
MIROC-ESM	Japan Agency for Marine-Earth Science and Technology, Atmosphere and Ocean Research Institute (The University of Tokyo), and National Institute for Environmental Studies
MIROC-ESM-CHEM	
MRI-CGCM3	Meteorological Research Institute

to access the prediction ability for the occurrence of new MPB mortality. Both evaluations were judged by the area under curve (AUC) of the receiver operating characteristics (ROC) curve, as well as overall accuracy (OA; Fielding & Bell, 1997; Hanley & McNeil, 1982). Overall accuracy was generated from the confusion matrix of the binary maps, where the probability of MPB mortality was separated from healthy forest with an optimal threshold calculated according to a criterion that maximizes the sum of sensitivity and specificity (Freeman & Moisen, 2008).

Projections under future climate scenarios

Future MPB mortality was projected using future climate conditions from the Coupled Model Intercomparison Project 5 (CMIP5). We used results from 14 global climate models (GCMs) downscaled to 4-km resolution by the Multivariate Adaptive Constructed Analogs (MACA) method, which was designed for wildfire applications in the western USA (Abatzoglou & Brown, 2012; Table 2). Projections under two future Representative Concentration Pathways, RCP4.5 and RCP8.5, have been adapted by MACA for downscaling. They represent a high pathway for which relative radiative forcing reaches >8.5 W/m^2 by 2100, and an intermediate pathway where radiative forcing is stabilized at 4.5 W/m^2 after 2100, separately. We made projections for each GCM and RCP, generated spatially-explicit maps, and calculated mean, 25th quartile, 75th quartile, lowest and highest probability of all GCM projections for each year and each RCP. Because data incorporating the climate change effects on the future forest extent and residential housing density at the spatial resolution of our model are not currently available, our projections assumed no changes in the distributions of forest and housing densities.

Results

In Liang et al. (2014), we reported that our Landsat-based change-detection analysis for mapping disturbances resulted in an overall accuracy (OA) ranging from 87% to 94%, which was 20–30% higher than single-scene classifications performed by a maximum likelihood classifier and an ensemble random forest classifier. Because of Landsat's medium resolution, the percentage of dead trees in one pixel can be variable. We visually interpreted the dead tree cover percentage on NAIP imagery within the 30 m pixel window of the test samples, and found that 90% of the MPB-mortality pixels had more than 50% dead tree cover, while 58% of them have more than 80% dead tree cover. Since the Landsat-derived MPB mortality data were used as observations when constructing our models, our results should be interpreted as explaining and predicting the spatiotemporal patterns of moderate to severe MPB mortality (>50% dead tree cover).

Sixteen out of 34 predictors had statistically significant coefficients at the 0.05 level as tested by univariate GLMs (Table 3), and none of the predictors produced models with spatially autocorrelated residuals except TWI. Residential housing density, all neighborhood mortality variables, mean temperature in the previous year, mean summer precipitation and maximum summer temperature, and winter mean temperature anomaly were positively related with MPB mortality. Negative relationships were found between MPB mortality and elevation, distance to MPB mortality in previous year, mean annual precipitation in the previous year, and mean summer precipitation.

Four predictor variables were retained in the full model after the backward stepwise selection (Table 3). Residential housing density, number of pixels in the nearest eight pixels that had MPB mortality in the previous year, and winter mean temperature anomaly were positively related to the likelihood of MPB mortality. Summer precipitation was also retained in the full model, but was negatively related to MPB mortality.

Besides quantifying the relative influence of the various drivers of MPB mortality, we were also curious about the predictive capacity of our GLM in a spatially explicit context. By assuming the satellite-derived disturbance maps were a true representation of landscape patterns of MPB mortality, we compared them against the GLM predictions for the validation years (Fig. 3). We observed that the predicted areas of MPB mortality generally matched well with the Landsat-based observations across the landscape. For instance, the northeast corner of Grand County is an area where the MPB outbreak progressively grew from 2006 to 2011. By carefully examining this zone, we found that the shrinking extent of healthy forests and the spread of MPB mortality as predicted by our model were basically in accordance with the satellite observed patterns. In the meantime, the areal estimates of MPB mortality predicted by the GLM for the whole county deviated little from the Landsat base maps, with 13% as the largest relative difference and the smallest relative difference was only 2%. Only year 2006 was under predicted and the remaining five independent validation years were over predicted. The annual predictions followed a pattern similar to that of the observed data (Fig. 4): both showed a steady increase in the amount of area with MPB mortality, with a more rapid rate of increase before 2008 and slower rate of change after that. In terms of quantitative evaluations, the average AUC generated from 10-fold cross-validation was 0.97, with small variation among years. Overall accuracy ranged from 82 to 93% and the average was 88% (Table 4). When we assessed accuracy only in areas of new MPB mortality each year, our model achieved a mean AUC of 0.72, a mean OA of 0.66.

Projections of future MPB mortality made with the GCM projections suggest that the MPB outbreak in Grand County would continue to spread until around year 2015 (Fig. 3, Fig. S1). The outbreak area predicted under the RCP8.5 scenario was consistently higher than that under RCP4.5. From 2015 to 2050, less variation existed in the projections among the GCMs and climate projections, as shown from the smaller difference between the upper and lower quartiles.

Table 3
Predictor variable coefficients and significance levels, and Moran's *I* for univariate general linear models (GLMs), and predictor variable coefficients and significance levels, and standard errors for the full multivariate GLM and the final multivariate GLM after stepwise selection. See Table 1 for explanations of the predictor variable abbreviations.

Variable abbreviation	Univariate GLMs		Multivariate GLM (full)		Multivariate GLM (final)	
	Coef	Moran's *I*	Coef	SE	Coef	SE
road	0.126	−0.026	0.396**	0.143		
house	1.089*	−0.034	1.258	0.661	1.198*	0.477
dem	−0.003**	−0.042	0.002	0.002		
aspect	0.041	−0.017	0.038	0.078		
slope	−0.026	−0.024	−0.026	0.025		
Sw	0.136	−0.017	0.140	0.264		
Twi	−1.104***	0.132*				
dis2chan	0.001	−0.019	0.000	0.004		
tc	−0.020	−0.025	−0.009	0.016		
dis2prev	−0.211***	−0.062	−0.070**	0.063		
nm_30m	0.582***	−0.028	0.660	0.205	0.642***	0.097
nm_100m	0.085***	−0.045	0.026	0.047		
nm_250m	0.010***	−0.053	−0.006	0.010		
nm_500m	0.002***	−0.050	0.001	0.003		
nm_1km	0.001**	−0.046	0.000	0.001		
nm_1500m	0.000*	−0.041	0.000	0.001		
nm_2km	0.000*	−0.039	0.002	0.002		
nm_3km	0.000*	−0.039	−0.003	0.003		
ppt_mean_last	−0.003**	−0.040	0.000	0.004		
tmean_last	0.405**	−0.046	11.880	7.005		
tmean_winter	0.132	−0.013	−5.131	3.280		
tmean_summer	0.246*	−0.031	−6.126*	3.619		
ppt_summer_cur	−0.014	−0.026	3.338*	36.820	−0.037**	0.014
ppt_summer_last	−0.011	−0.029	−3.395	36.820		
tmin_cur	−0.014	−0.021	0.048	0.786		
tmax_cur	0.155**	−0.026	−0.384	0.870		
ppt_mean_last2normal	0.000	−0.020	−0.018	0.010		
tmean_last2normal	−0.529	−0.012	−13.10	7.173		
tmean_winter2normal	0.030	−0.018	6.801	3.404	0.659**	0.205
tmean_summer2normal	−0.043	−0.021	8.662	3.800		
ppt_summer_cur2normal	0.002	−0.020	−3.388	36.820		
ppt_summer_last2normal	0.005	−0.019	3.459	36.820		
tmin_cur2normal	0.033	−0.017	−0.313	0.794		
tmax_cur2normal	−0.005	−0.020	−1.575	1.087		
(intercept)			15.330	19.340	0.460	0.652

Note: coef – coefficient estimate on the variable; SE – standard error; * denotes significance level of 0.05; ** denotes significance level of 0.01; and *** denotes significance level of 0.001.

Discussion

Our Landsat-derived disturbance maps documented an evolving pattern where a severe MPB outbreak emerged in the early 2000s, spread throughout the decade with the population reaching epidemic levels and peak mortality around 2006. Based on that historical record of forest disturbance (Liang et al., 2014), and the models developed in this study, our research provided a means of simulating the landscape-level outbreak pattern over time. The major controls on the observed patterns of MPB mortality during the time period of this study included residential housing density, density of adjacent MPB mortality in previous years, and climate predictors. The diversity of predictor variables indicated the complexity in predicting the incidence of MPB mortality. Given future climate projections, and an assumption that other controlling factors, such as the supply of nutritionally optimal host trees (Raffa et al., 2008), we anticipate that landscape-level outbreak will become more extensive and severe.

Detecting spatiotemporal changes in MPB activity and associated uncertainties

During the course of this study, we experienced challenges in obtaining an ideal dataset that accurately depicted the dynamic extent of MPB mortality at a landscape scale because of the heterogenous nature of MPB outbreaks. Mortality is rarely complete within forest plots, stands, and/or pixel-level satellite observations. Healthy trees are often found next to attacked trees and attacked trees can be present in various stages of mortality (e.g., red, gray). In addition to those issues, data with high levels of omission and/or commission errors should be avoided for use in descriptive and predictive models as they may result in false inferences being made about the underlying mechanisms influencing patterns of MPB mortality and result in erroneous predictions. However, there are very few publicly available data describing the spatial and temporal patterns of MPB mortality, and most studies predicting patterns of beetle occurrence collected their response variables via field work, ADS, or image interpretation. Among these, ADS has been used more widely because of its availability and information richness, such as host species and type of disturbance agent (Hicke, Meddens, Allen, & Kolden, 2013; Meddens, Hicke, & Ferguson, 2012; Preisler et al., 2012; Strohm, Tyson, & Powell, 2013), but the subjective nature and the limited spatiotemporal extent of the ADS data made their integration in our analysis problematic (Hicke et al., 2012). Johnson and Ross (2008) suggested that the accuracy of ADS data is most acceptable for coarse-scale (>500 m) studies, and less suitable at intermediate scales (>50 m), and should be cautiously used at fine spatial scales. We also lacked enough time-series samples in the disturbed areas to conduct a quantitative evaluation of the ADS data. Nonetheless, our visual examination suggested that there are substantial duplications in areas of mortality sketch mapped among different years and that the fine-scale

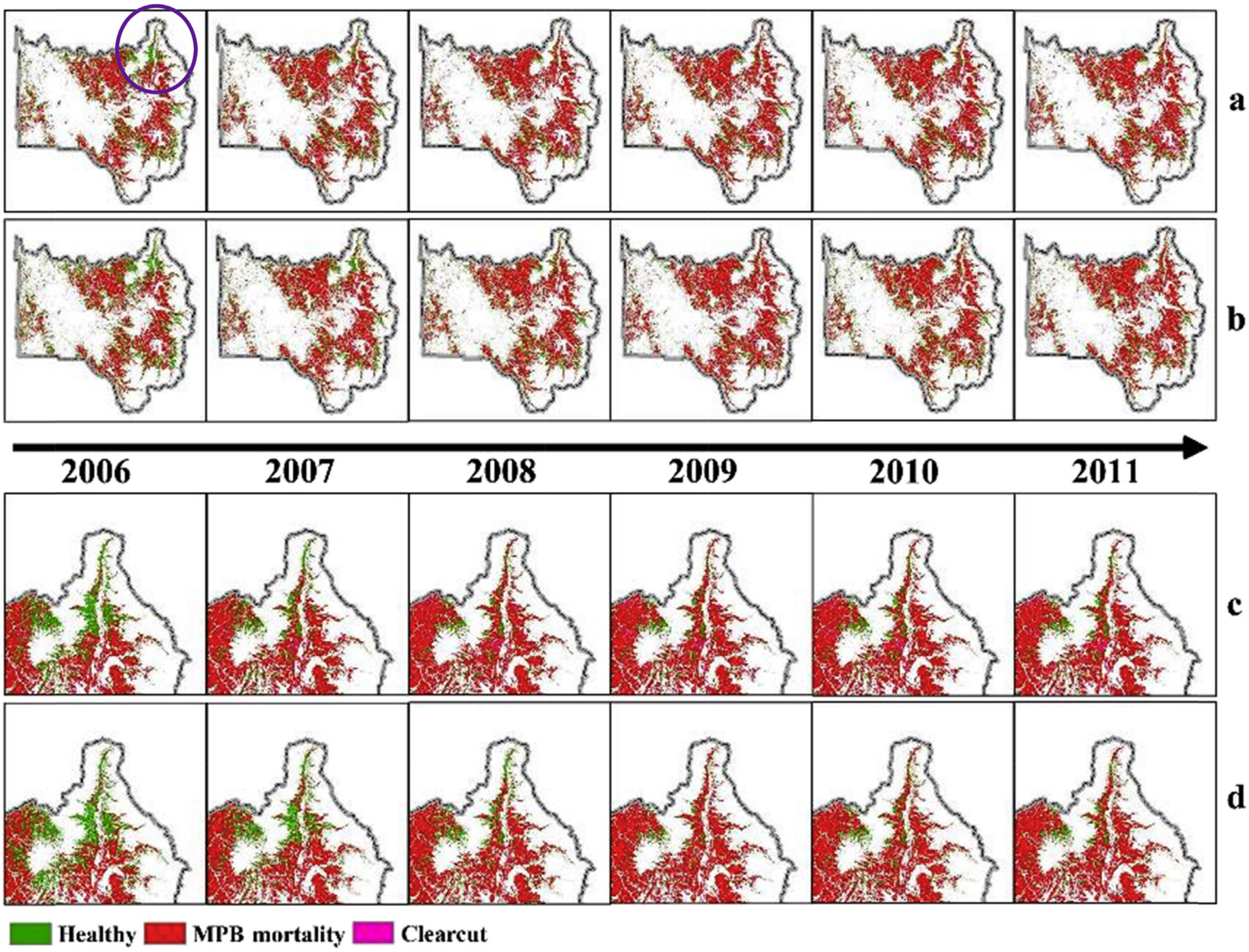

Fig. 3. The comparison between observed disturbances in the change-detection analysis (panels a, c) and predictions of MPB mortality using the final GLM (panels b, d) in the independent validation years. Panels c and d show the detailed images from the northeast corner of the study area, the area of which is indicated by the circle in the leftmost panel a.

heterogenous patterns of MPB outbreaks are not well characterized. Thus, future studies that utilize the ADS data should incorporate methods to assess their uncertainties and the impacts they have on analyses relying upon them.

Instead of relying on the ADS data, we implemented our own algorithm to track and identify forest disturbances with Landsat data (Liang et al., 2014). Our method built upon the LandTrendr algorithm (Kennedy et al., 2010), but incorporated methods to

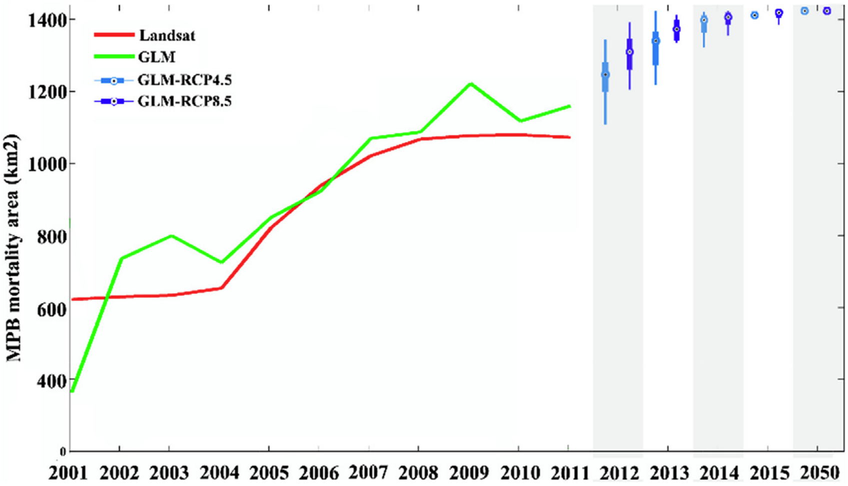

Fig. 4. Accumulated area of mountain pine beetle (MPB) mortality detected by Landsat and predicted by our general linear model from 2001 to 2011, as well as forecasted MPB mortality to 2050.

Table 4
Comparison of the final general linear model (GLM) results to Landsat observed disturbances.

		AA1		AA2		Landsat (km^2)	GLM (km^2)	RD
		AUC	OA	AUC	OA			
Training period	2000–2005	0.98	0.87			833.23	861.62	0.03
Validation years	2006	0.94	0.89	0.67	0.63	950.03	934.55	−0.02
	2007	0.96	0.87	0.63	0.58	1031.18	1079.10	0.05
	2008	0.97	0.91	0.66	0.57	1077.13	1096.70	0.02
	2009	0.98	0.82	0.77	0.73	1087.08	1230.60	0.13
	2010	0.98	0.93	0.79	0.73	1088.95	1126.70	0.03
	2011	0.98	0.87	0.80	0.71	1082.05	1168.40	0.08

AA1: accuracy assessment on the predicted annual image (previous year's + new mortality area); AA2: accuracy assessment on the predicted newly emerged mortality areas. For training period, the accuracy is tested by the 10-fold cross-validation. AUC: area under the curve of a receiver operating characteristic plot. OA: overall accuracy.

automatically label changed areas identified by LandTrendr with the type of disturbance causing the change. The change detection analysis disturbance maps used in this study showed promising results, especially in their ability to produce long-term time series of insect mortality. Our next steps will pursue testing and application of the change detection analysis for disturbance mapping at greater spatial extents. There have been several efforts in providing the broad patterns of forest dynamics across the continent, e.g., the North American Forest Dynamics project (Masek et al., 2013), and a recent 30-m resolution global forest change product (Hansen et al., 2013), but the lack of information identifying specific disturbance types limits their usability in studies identifying the drivers behind the change. Meanwhile, errors from our mapping procedure may have affected the accuracy and applicability of the subsequent models. For instance, in the accuracy assessment, we found that although the overall accuracy was as high as 90%, the commission errors of MPB mortality were higher than omission errors by an average of 10%, and higher omission errors were found in the clearcut land cover type (Liang et al., 2014). This might have resulted in sampling errors that were propagated in the GLM results.

Driving factors of the dynamic beetle infestation pattern

Residential housing density, beetle pressure and climate were key predictors in the final model after stepwise selection, which reflects the effects of human impacts, biological dispersal and physical environmental factors in MPB outbreaks. Except for housing density, the function of the other key variables in driving beetle outbreaks has already been highlighted in some previous studies. For instance, Preisler et al. (2012) found beetle pressure, minimum winter temperature, and two-year cumulative precipitation to be important predictors of MPB-caused tree mortality. The positive effect of residential housing density on MPB mortality indicated that anthropogenic influences provide a positive feedback to beetle outbreaks. We suspect that the positive association exists for two reasons. First, tree removal resulting from hazard mitigation, timber harvesting, and recreational facility construction such as ski resorts is common in Grand County. Increasing fragmentation of remaining forests, leaving them with higher edge-to-area ratios (Raffa et al., 2008) and drier conditions because of higher levels of solar radiation (Bone, White, Wulder, Robertson, & Nelson, 2013). Consequently, those forests are more likely to be exposed to mass attack by MPB. Second, modern urban environments have greatly altered soil physical and biochemical properties and heavier pollutant loads, all of which could hamper tree growth and make them more susceptible to insect attacks (Bone et al., 2013).

The importance of the number of adjacent pixels with MPB mortality in the previous year in predicting MPB mortality in our models is in agreement with the current understanding of MPB population dynamics (Aukema et al., 2008; Walter & Platt, 2013). Greater MPB densities allow for mass attack and increase the likelihood of tree mortality regardless of the vigor and defense system of host trees. Simard et al. (2012) demonstrated that the amount of beetle-killed forest in adjacent areas was a key predictor of subsequent mortality, and that beetle density is also a potentially factor limiting stand-scale outbreaks from developing into landscape-scale outbreaks (Raffa et al., 2008). Meanwhile, we observed that among all the eight neighborhood mortality variables, only nm_30m was retained in the final GLM model, which indicated to us that short-distance dispersal was the dominant mode of expansion of the MPB outbreak in Grand County. Long-distance dispersal has been suggested to be crucial in the initiation and early stages of infestations, but short-distance dispersal dominates the stage when infestations intensify and populations reach epidemic levels (Chen & Walton, 2011). Our starting year was 2000, at which time MPB had already formed two outbreak clusters in the northern and southern corners of our study area. Because of the relatively important role of the short-distance dispersal, it is not surprising that we observed and predicted a continuously expanding pattern of MPB mortality in subsequent years instead of isolated MPB infestations.

Our study also identified a negative relationship with summer precipitation and a positive relationship with winter temperature and MPB mortality. These relationships have also been found by other studies; higher temperatures foster outbreaks whereas lower temperatures depress beetle populations (Bentz et al., 2010; Kaufmann et al., 2008; Raffa et al., 2008). A warmer climate will reduce the cold-induced mortality in the adult and larval stages, and will accelerate the developmental timing within one generation. The thermal changes can also determine the abundance of the fungal species vectored by MPB (Six & Bentz, 2007), which will ultimately affect the success of MPB populations. The association between precipitation and MPB mortality is less understood than the relationships with temperature. Preisler et al. (2012) found that precipitation in the previous year increased the odds of outbreak intensification, which could be related to the increased beetle brood production within thicker phloem. In contrast, longer drought periods may lead to increased host susceptibility and thus result in a higher probability of outbreak intensification. The negative effect of summer precipitation as indicated from our study supports the latter statement.

Conclusion

Evidence has been accumulating to document the contribution of climate change to recent increases in the frequency, duration, extent, and severity of insect disturbances (Kurz et al., 2008). Despite uncertainty in downscaled forecasts of future climate elements, both the RCP 4.5 and 8.5 climate-change scenarios indicated an expanding extent of MPB mortality, with the implication that future climate conditions in Grand County, Colorado will be more suitable for MPB survival. Little variation existed in the projected area of MPB mortality in Grand County between years 2015 and 2050, because a limited amount of healthy forest with MPB host species may remain at that point. Because of this, our projections for Grand County do not fully depict the situation in the Southern Rocky Mountains ecoregion, as there is a substantial amount of lodgepole and other species of pine forests that currently remain healthy outside of Grand County. Given that projected climate conditions within the ecoregion are likely to follow those within Grand County, we anticipate the area of forest with MPB mortality within the ecoregion will increase. The influence of climate and weather factors on the beetle-caused tree mortality varies among different locations (Creeden et al., 2014), and not all areas across western North America are expected to be more suitable to MPB survival as temperatures increase (Hicke et al., 2006). Thus, the models developed, and the conclusions drawn from this study might not be applicable to other areas. However, our overall approach is applicable to other regions experiencing similar insect outbreaks and can aid in generating consistent and high-temporal frequency data on insect mortality and other disturbances impacting carbon cycling and other ecosystem services.

Acknowledgments

This research was supported by the U.S. Geological Survey, Climate and Land Use Mission Area Land Change Science Program (grant number G12AC20085), and a National High Technology Grant from China (2009AA12200101). We also would like to acknowledge the World Climate Research Programme's Working Group on Coupled Modelling, which is responsible for CMIP, and we thank the climate modeling groups (listed in Table 2 of this paper) for producing and making available their model output. For CMIP, the U.S. Department of Energy's Program for Climate Model Diagnosis and Intercomparison provides coordinating support and led development of software infrastructure in partnership with the Global Organization for Earth System Science Portals. Two anonymous reviewers, Diane Stephens and Julie Ann Beston provided insightful comments on a previous draft of this manuscript and their comments helped greatly to improve the completeness and clarity of the manuscript. Any use of trade, firm, or product names is for descriptive purposes only and does not imply endorsement by the U.S. Government.

Appendix A. Supplementary data

Supplementary data related to this article can be found at http://dx.doi.org/10.1016/j.apgeog.2014.09.012.

References

Abatzoglou, J. T., & Brown, T. J. (2012). A comparison of statistical downscaling methods suited for wildfire applications. *International Journal of Climatology, 32*, 772–780.

Amman, G. D. (1977). The role of mountain pine beetle in lodgepole ecosystems, impact on succession. In W. J. Mattson (Ed.), *The role of arthropods in forest ecosystem*. New York: Springer-Verlag.

Amman, G. D., & Cole, W. E. (1983). *Mountain pine beetle dynamics in lodgepole pine forests. Part II: Population dynamics*. General technical report. Intermountain Forest and Range Experiment Station, USDA Forest Service.

Aukema, B. H., Carroll, A. L., Zheng, Y., Zhu, J., Raffa, K. F., Dan Moore, R., et al. (2008). Movement of outbreak populations of mountain pine beetle: influences of spatiotemporal patterns and climate. *Ecography, 31*, 348–358.

Aukema, B. H., Carroll, A. L., Zhu, J., Raffa, K. F., Sickley, T. A., & Taylor, S. W. (2006). Landscape level analysis of mountain pine beetle in British Columbia, Canada: spatiotemporal development and spatial synchrony within the present outbreak. *Ecography, 29*, 427–441.

Baker, W. L., & Veblen, T. T. (1990). Spruce beetles and fires in the nineteenth-century subalpine forests of western Colorado, U.S.A. *Arctic and Alpine Research, 22*, 65–80.

Bentz, B. J., Régnière, J., Fettig, C. J., Hansen, E. M., Hayes, J. L., Hicke, J. A., et al. (2010). Climate change and bark beetles of the western United States and Canada: direct and indirect effects. *BioScience, 60*, 602–613.

Beven, K., & Kirkby, M. J. (1979). A physically based, variable contributing area model of basin hydrology [Un modèle à base physique de zone d'appel variable de l'hydrologie du bassin versant]. *Hydrological Sciences Journal, 24*, 43–69.

Bone, C., White, J. C., Wulder, M. A., Robertson, C., & Nelson, T. A. (2013). Impact of forest fragmentation on patterns of mountain pine beetle-caused tree mortality. *Forests, 4*, 279–295.

Boon, S. (2009). Snow ablation energy balance in a dead forest stand. *Hydrological Processes, 23*, 2600–2610.

Caldwell, M., Hawbaker, T., Briggs, J., Cigan, P., & Stitt, S. (2013). Simulated impacts of mountain pine beetle and wildfire disturbances on forest vegetation composition and carbon stocks in the Southern Rocky Mountains. *Biogeosciences, 10*, 12919–12965.

Chen, H. P., & Walton, A. (2011). Mountain pine beetle dispersal: spatiotemporal patterns and role in the spread and expansion of the present outbreak. *Ecosphere, 2*. art66.

Collins, B. J., Rhoades, C. C., Hubbard, R. M., & Battaglia, M. A. (2011). Tree regeneration and future stand development after bark beetle infestation and harvesting in Colorado lodgepole pine stands. *Forest Ecology and Management, 261*, 2168–2175.

Coops, N. C., Timko, J. A., Wulder, M. A., White, J. C., & Ortlepp, S. M. (2008). Investigating the effectiveness of mountain pine beetle mitigation strategies. *International Journal of Pest Management, 54*, 151–165.

Coops, N. C., Wulder, M. A., & White, J. C. (2006). Integrating remotely sensed and ancillary data sources to characterize a mountain pine beetle infestation. *Remote Sensing of Environment, 105*, 83–97.

Creeden, E. P., Hicke, J. A., & Buotte, P. C. (2014). Climate, weather, and recent mountain pine beetle outbreaks in the western United States. *Forest Ecology and Management, 312*, 239–251.

Daly, C., Gibson, W. P., Taylor, G. H., Johnson, G. L., & Pasteris, P. (2002). A knowledge-based approach to the statistical mapping of climate. *Climate Research, 22*, 99–113.

Dormann, F. C., McPherson, J. M., Araújo, M. B., Bivand, R., Bolliger, J., Carl, G., et al. (2007). Methods to account for spatial autocorrelation in the analysis of species distributional data: a review. *Ecography, 30*, 609–628.

Edburg, S. L., Hicke, J. A., Brooks, P. D., Pendall, E. G., Ewers, B. E., Norton, U., et al. (2012). Cascading impacts of bark beetle-caused tree mortality on coupled biogeophysical and biogeochemical processes. *Frontiers in Ecology and the Environment, 10*, 416–424.

Evangelista, P. H., Kumar, S., Stohlgren, T. J., & Young, N. E. (2011). Assessing forest vulnerability and the potential distribution of pine beetles under current and future climate scenarios in the Interior West of the US. *Forest Ecology and Management, 262*, 307–316.

Evenden, M. L., Whitehouse, C. M., & Sykes, J. (2014). Factors influencing flight capacity of the mountain pine beetle (Coleoptera: Curculionidae: Scolytinae). *Environmental Entomology, 43*, 187–196.

Fielding, A. H., & Bell, J. F. (1997). A review of methods for the assessment of prediction errors in conservation presence/absence models. *Environmental Conservation, 24*, 38–49.

Franklin, J., McCullough, P., & Gray, C. (2000). *Terrain variables used for predictive mapping of vegetation communities in Southern California. Terrain analysis: Principles and applications*.

Freeman, E. A., & Moisen, G. (2008). PresenceAbsence: an R package for presence absence analysis. *Journal of Statistical Software, 23*, 1–31.

Gill, S. J., Biging, G. S., & Murphy, E. C. (2000). Modeling conifer tree crown radius and estimating canopy cover. *Forest Ecology and Management, 126*, 405–416.

de la Giroday, H. M. C., Carroll, A. L., Lindgren, B. S., & Aukema, B. H. (2011). Incoming! Association of landscape features with dispersing mountain pine beetle populations during a range expansion event in western Canada. *Landscape Ecology, 26*, 1097–1110.

Grand County Department of Natural Resources. (2006). *Grand County Community wildfire protection plan*.

Hanley, J. A., & McNeil, B. J. (1982). The meaning and use of the area under a receiver operating characteristic (ROC) curve. *Radiology, 143*, 29–36.

Hansen, M., Potapov, P., Moore, R., Hancher, M., Turubanova, S., Tyukavina, A., et al. (2013). High-resolution global maps of 21st-century forest cover change. *Science, 342*, 850–853.

Hicke, J. A., Allen, C. D., Desai, A. R., Dietze, M. C., Hall, R. J., Kashian, D. M., et al. (2012). Effects of biotic disturbances on forest carbon cycling in the United States and Canada. *Global Change Biology, 18*, 7–34.

Hicke, J. A., Logan, J. A., Powell, J., & Ojima, D. S. (2006). Changing temperatures influence suitability of modeled mountain pine beetle (*Dendroctonus ponderosae*) outbreaks in the western United States. *Journal of Geophysical Research, 111*, G02019. http://dx.doi.org/10.1029/2005JG000101.

Hicke, J. A., Meddens, A. J., Allen, C. D., & Kolden, C. A. (2013). Carbon stocks of trees killed by bark beetles and wildfire in the western United States. *Environmental Research Letters, 8*, 035032.

Huang, C., Goward, S. N., Masek, J. G., Thomas, N., Zhu, Z., & Vogelmann, J. E. (2010). An automated approach for reconstructing recent forest disturbance history using dense Landsat time series stacks. *Remote Sensing of Environment, 114*, 183–198.

Jackson, P. L., Straussfogel, D., Lindgren, B. S., Mitchell, S., & Murphy, B. (2008). Radar observation and aerial capture of mountain pine beetle, *Dendroctonus ponderosae* Hopk. (Coleoptera: Scolytidae) in flight above the forest canopy. *Canadian Journal of Forest Research, 38*, 2313–2327.

Jenkins, M. J., Hebertson, E., Page, W., & Jorgensen, C. A. (2008). Bark beetles, fuels, fires and implications for forest management in the Intermountain West. *Forest Ecology and Management, 254*, 16–34.

Johnson, E. W., & Ross, J. (2008). Quantifying error in aerial survey data. *Australian Forestry, 71*, 216–222.

Kaufmann, M. R., Aplet, G. H., Babler, M. G., Baker, W. L., Bentz, B., Harrington, M., et al. (2008). *The status of our scientific understanding of lodgepole pine and mountain pine beetles: A focus on forest ecology and fire behavior*. Arlington, VA: Nature Conservancy.

Kennedy, R. E., Yang, Z., & Cohen, W. B. (2010). Detecting trends in forest disturbance and recovery using yearly Landsat time series: 1. LandTrendr—temporal segmentation algorithms. *Remote Sensing of Environment, 114*, 2897–2910.

Key, C. H., & Benson, N. C. (2006). *Landscape assessment (LA). FIREMON: Fire effects monitoring and inventory system*. Gen. Tech. Rep. RMRS-GTR-164-CD. Fort Collins, CO: US Department of Agriculture, Forest Service, Rocky Mountain Research Station.

Klutsch, J. G., Negron, J. F., Costello, S. L., Rhoades, C. C., West, D. R., Popp, J., et al. (2009). Stand characteristics and downed woody debris accumulations associated with a mountain pine beetle (*Dendroctonus ponderosae* Hopkins) outbreak in Colorado. *Forest Ecology and Management, 258*, 641–649.

Kurz, W. A., Dymond, C., Stinson, G., Rampley, G., Neilson, E., Carroll, A., et al. (2008). Mountain pine beetle and forest carbon feedback to climate change. *Nature, 452*, 987–990.

Liang, L., Chen, Y., Hawbaker, T. J., Zhu, Z., & Gong, P. (2014). Mapping mountain pine beetle mortality through growth trend analysis of time-series Landsat data. *Remote Sensing, 6*, 5696–5716.

Man, G. (2010). *Major forest insect and disease conditions in the United States: 2009 Update*. Washington: US Department of Agriculture, Forest Service, Forest Health Protection.

Maness, H., Kushner, P., & Fung, I. (2013). Summertime climate response to mountain pine beetle disturbance in British Columbia. *Nature Geoscience, 6*, 65–70.

Manly, B., McDonald, L., Thomas, D., McDonald, T., & Erickson, W. (2002). *Resource selection by animals: Statistical analysis and design for field studies*. Nordrecht, The Netherlands: Kluwer.

Masek, J. G., Goward, S. N., Kennedy, R. E., Cohen, W. B., Moisen, G. G., Schleweiss, K., et al. (2013). United States forest disturbance trends observed with Landsat time series. *Ecosystems, 16*, 1087–1104.

Meddens, A. J., Hicke, J. A., & Ferguson, C. A. (2012). Spatiotemporal patterns of observed bark beetle-caused tree mortality in British Columbia and the western United States. *Ecological Applications, 22*, 1876–1891.

Meddens, A. J., Hicke, J. A., Vierling, L. A., & Hudak, A. T. (2013). Evaluating methods to detect bark beetle-caused tree mortality using single-date and multi-date Landsat imagery. *Remote Sensing of Environment, 132*, 49–58.

Meigs, G. W., Kennedy, R. E., & Cohen, W. B. (2011). A Landsat time series approach to characterize bark beetle and defoliator impacts on tree mortality and surface fuels in conifer forests. *Remote Sensing of Environment, 115*, 3707–3718.

Mikkelson, K. M., Bearup, L. A., Maxwell, R. M., Stednick, J. D., McCray, J. E., & Sharp, J. O. (2013). Bark beetle infestation impacts on nutrient cycling, water quality and interdependent hydrological effects. *Biogeochemistry, 115*, 1–21.

Moran, P. A. P. (1950). Notes on continuous stochastic phenomena. *Biometrika, 37*, 17–23.

Parker, T. J., Clancy, K. M., & Mathiasen, R. L. (2006). Interactions among fire, insects and pathogens in coniferous forests of the interior western United States and Canada. *Agricultural and Forest Entomology, 8*, 167–189.

Preisler, H. K., Hicke, J. A., Ager, A. A., & Hayes, J. L. (2012). Climate and weather influences on spatial temporal patterns of mountain pine beetle populations in Washington and Oregon. *Ecology, 93*, 2421–2434.

PRISM Climate Group. (2010). Gridded climate data for the contiguous USA. http://prism.oregonstate.edu.

Radeloff, V. C., Stewart, S. I., Hawbaker, T. J., Gimmi, U., Pidgeon, A. M., Flather, C. H., et al. (2010). Housing growth in and near United States protected areas limits their conservation value. *Proceedings of the National Academy of Sciences of the United States of America, 107*, 940–945.

Raffa, K. F., Aukema, B. H., Bentz, B. J., Carroll, A. L., Hicke, J. A., Turner, M. G., et al. (2008). Cross-scale drivers of natural disturbances prone to anthropogenic amplification: the dynamics of bark beetle eruptions. *Bioscience, 58*, 501–517.

Raffa, K. F., & Berryman, A. A. (1983). The role of host plant resistance in the colonization behavior and ecology of bark beetles (Coleoptera: Scolytidae). *Ecological Monographs, 53*, 27–49.

R Core Team. (2013). *R: A language and environment for statistical computing*. R Foundation for Statistical Computing.

Robertson, C., Nelson, T. A., & Boots, B. (2007). Mountain pine beetle dispersal: the spatial–temporal interaction of infestations. *Forest Science, 53*, 395–405.

Robertson, C., Nelson, T. A., Jelinski, D. E., Wulder, M. A., & Boots, B. (2009). Spatial–temporal analysis of species range expansion: the case of the mountain pine beetle, *Dendroctonus ponderosae*. *Journal of Biogeography, 36*, 1446–1458.

Robertson, C., Wulder, M. A., Nelson, T. A., & White, J. C. (2008). Risk rating for mountain pine beetle infestation of lodgepole pine forests over large areas with ordinal regression modelling. *Forest Ecology and Management, 256*, 900–912.

Running, S. W. (2008). Ecosystem disturbance, carbon, and climate. *Science, 321*, 652–653.

Safranyik, L., Linton, D. A., Silversides, R., & McMullen, L. H. (1992). Dispersal of released mountain pine beetles under the canopy of a mature lodgepole pine stand. *Journal of Applied Entomology, 113*, 441–450.

Safranyik, L., Silversides, R., McMullen, L. H., & Linton, D. A. (1989). An empirical approach to modeling the local dispersal of the mountain pine beetle (*Dendroctonus ponderosae* Hopk.) (Col., Scolytidae) in relation to sources of attraction, wind direction and speed. *Journal of Applied Entomology, 108*, 498–511.

Schoennagel, T., Veblen, T. T., Negron, J. F., & Smith, J. M. (2012). Effects of mountain pine beetle on fuels and expected fire behavior in lodgepole pine forests, Colorado, USA. *PLoS One, 7*, e30002.

Sexton, J. O., Song, X.-P., Feng, M., Noojipady, P., Anand, A., Huang, C., et al. (2013). Global, 30-m resolution continuous fields of tree cover: Landsat-based rescaling of MODIS vegetation continuous fields with lidar-based estimates of error. *International Journal of Digital Earth, 6*, 427–448.

Simard, M., Powell, E. N., Raffa, K. F., & Turner, M. G. (2012). What explains landscape patterns of tree mortality caused by bark beetle outbreaks in Greater Yellowstone? *Global Ecology and Biogeography, 21*, 556–567.

Six, D., & Bentz, B. (2007). Temperature determines symbiont abundance in a multipartite bark beetle–fungus ectosymbiosis. *Microbial Ecology, 54*, 112–118.

Strohm, S., Tyson, R., & Powell, J. (2013). Pattern formation in a model for mountain pine beetle dispersal: linking model predictions to data. *Bulletin of Mathematical Biology, 75*, 1778–1797.

USGS. (2004). *Shuttle radar topography mission, 1 arc second scene SRTM_u03_n008e004, unfilled unfinished 2.0*. College Park, Maryland: Global Land Cover Facility, University of Maryland. February 2000.

Walter, J. A., & Platt, R. V. (2013). Multi-temporal analysis reveals that predictors of mountain pine beetle infestation change during outbreak cycles. *Forest Ecology and Management, 302*, 308–318.

Watts, R. D., Compton, R. W., McCammon, J. H., Rich, C. L., Wright, S. M., Owens, T., et al. (2007). Roadless space of the conterminous United States. *Science, 316*, 736–738.

White, J. C., Wulder, M. A., Brooks, D., Reich, R., & Wheate, R. D. (2004). Mapping mountain pine beetle infestation with high spatial resolution satellite imagery. *The Forestry Chronicle, 80*, 743–745.

Witcosky, J. (2007). *Status of mountain pine beetle populations in lodgepole pine stands in northern Colorado and southern Wyoming*. USDA Forest Service, Rocky Mountain Region, Forest Health Management, Lakewood Service Center. LSC-07-06.

Wulder, M. A., White, J., Bentz, B., Alvarez, M., & Coops, N. (2006). Estimating the probability of mountain pine beetle red-attack damage. *Remote Sensing of Environment, 101*, 150–166.